IJARSCT
International Journal of Advanced Research in Science, Communication and Technology
International Open-Access, Double-Blind, Peer-Reviewed, Refereed, Multidisciplinary Online Journal
ISSN: 2581-9429
Volume 6, Issue 2, May 2026
Impact Factor: 8.2

Design and Development of a LoRa-Based IoT Network for Smart Applications

Y. G. Bachhav[1], S. S. Mogal[2], S. S. Shinde[3], V. R. Kadam[4], S. G. Bagul[5]
Department of Electronics and Telecommunication Engineering
Late G. N. Sapkal College of Engineering, Nashik, India (Affiliated to SPPU)[12345]
Bachhavyash15@gmail.com[1],shivammogal110@gmail.com[2],shindeshubham7498@gmail.com[3],
vaishalikadam9094@gmail.com[4], sachinbagul1985@gmail.com[5]

Abstract: *Monitoring environmental hazards such as rising water levels and combustible gas leakage in real time remains a critical challenge in remote and infrastructure-limited areas. Conventional wireless technologies like Wi-Fi and cellular networks are often impractical in such settings due to high power demands and dependence on existing infrastructure. This paper presents the design, implementation, and field testing of a LoRa based IoT network built around ESP32 microcontrollers and RYLR998 transceiver modules, operating at 865 MHz under India's ISM band regulations. The transmitter node acquires water-level data via an HC-SR04 ultrasonic sensor and gas concentration data via an MQ-2 metal oxide semiconductor sensor. Both readings are packaged into structured packets and transmitted wirelessly to a gateway receiver node. The gateway decodes incoming data, displays it on a 16×2 I2C LCD, forwards readings to the Blynk IoT cloud platform, and activates an audible buzzer whenever values exceed predefined safety thresholds. Field tests across three environments — indoor (30 m), open field (500 m), and semi-urban (1 km) — achieved packet delivery ratios of 99.6%, 97.8%, and 95.3% respectively, with end-to-end latency below 380 ms throughout. Hardware integration challenges, including UART configuration, I2C address conflicts, and GPIO voltage compatibility, are documented as an engineering reference..*

Keywords: LoRa, IoT, ESP32, RYLR998, LPWAN, Smart Monitoring, Blynk, Packet Delivery Ratio, 865 MHz ISM Band

I. INTRODUCTION

In recent years, the rapid expansion of the Internet of Things (IoT) has opened new possibilities for automating the monitoring of physical environments. From industrial facilities to remote agricultural fields, the ability to continuously track conditions such as water levels and gas concentrations without human presence has become increasingly valuable. However, deploying such systems in locations that lack reliable internet or cellular coverage remains a significant practical challenge.

Conventional short-range wireless technologies such as Wi Fi and Bluetooth, while widely available, are unsuitable for deployments beyond a few tens of meters. Cellular networks offer broader coverage but introduce ongoing subscription costs and depend on operator infrastructure that may be absent in rural or semi-urban areas. These limitations create a clear need for a communication technology that balances long range, low power consumption, and infrastructure independence.

LoRa (Long Range) modulation, developed by Semtech Corporation using the Chirp Spread Spectrum (CSS) technique, addresses these requirements effectively. It enables communication over several kilometres with minimal power consumption, operating entirely in the unlicensed ISM band without any subscription fee [1]. In India, the designated ISM band for LoRa operation falls between 865 MHz and 867 MHz, which is the frequency range adopted in this work.

Copyright to IJARSCT
www.ijarsct.co.in
DOI: 10.48175/IJARSCT-34877

IJARSCT
International Journal of Advanced Research in Science, Communication and Technology
International Open-Access, Double-Blind, Peer-Reviewed, Refereed, Multidisciplinary Online Journal
ISSN: 2581-9429 Volume 6, Issue 2, May 2026 Impact Factor: 8.2

Despite the growing body of research on LoRa-based systems, most published implementations focus on a single sensing parameter and rely solely on cloud platforms for monitoring. This creates two practical weaknesses: inability to capture multiple environmental hazards simultaneously, and dependency on network connectivity for alerts [4]. A robust monitoring system must support multi-parameter sensing and provide reliable alert mechanisms independent of network availability.

This paper addresses these gaps by presenting the design and development of a two-node LoRa-based IoT network that integrates water-level monitoring and gas-hazard detection within a single architecture. The transmitter node, built around an ESP32 microcontroller, reads an HC-SR04 ultrasonic sensor for water level and an MQ-2 gas sensor for gas concentration, then wirelessly transmits the combined readings via the RYLR998 LoRa module. The gateway receiver decodes in coming packets and delivers output through three independent channels a 16×2 I2C LCD display, a threshold-triggered active buzzer, and the Blynk IoT cloud platform ensuring that safety alerts reach the operator regardless of network availability.

The key contributions of this work are as follows:

- A validated dual-parameter IoT system combining ultrasonic water-level sensing and gas detection over a single LoRa link.
- A tri-modal alerting architecture that operates independently of internet connectivity, ensuring uninterrupted safety monitoring.
- Experimental performance evaluation across multiple environments, reporting PDR, RSSI, SNR, and latency.
- Documentation of hardware integration challenges for practical implementation reference.
- A complete component-level cost and power consumption analysis for Indian ISM-band deployments.

II. LITERATURE REVIEW

The evolution of IoT communication technologies has been extensively studied over the past decade, with particular focus on finding solutions that balance range, power consumption, and deployment cost. This section reviews key works that form the foundation of the present study.

Semtech Corporation [1] introduced LoRa modulation based on Chirp Spread Spectrum (CSS), demonstrating that reliable signal recovery is achievable even at power levels well below the ambient noise floor. A critical insight from this work is that the Spreading Factor (SF) parameter directly controls the trade-off between communication range and data throughput —a principle that guided the selection of SF9 in the present system.

Augustin et al. [2] conducted one of the earliest comprehensive studies of LoRa network behaviour, examining how parameters such as bandwidth, coding rate, and spreading factor interact to determine link performance. Their findings confirmed that increasing the spreading factor extends coverage at the cost of longer transmission time, which directly informed the configuration choices made in this work.

Raza et al. [3] carried out a broad comparison of LPWAN technologies including LoRa, Sigfox, and NB-IoT, concluding that LoRa offers the most flexibility for private network deployments where dedicated gateway infrastructure is not feasible. This supports the peer-to-peer LoRa architecture adopted in the proposed system.

Liando et al. [4] performed a large-scale evaluation of LoRa networks in urban environments, identifying multipath fading and duty-cycle restrictions as the primary factors responsible for packet loss. Their reported PDR values of 90–97% across varying spreading factors provide a meaningful benchmark for the performance results presented in Section VI.

Islam et al. [5] demonstrated an IoT-based water-level monitoring system using a JSN-SR04T ultrasonic sensor paired with a LoRa SX1276 module on an ESP32 platform. While their work validated the concept of LoRa-based level sensing, it was limited to a single parameter and did not incorporate local alerting or cloud-based monitoring, both of which are addressed in the present architecture.

Shanmuga Sundaram et al. [6] surveyed open research challenges in LoRa networking, with particular attention to MAC layer collision avoidance and coverage optimisation in multi node deployments. Their analysis highlighted the

IJARSCT
International Journal of Advanced Research in Science, Communication and Technology
International Open-Access, Double-Blind, Peer-Reviewed, Refereed, Multidisciplinary Online Journal
ISSN: 2581-9429
Volume 6, Issue 2, May 2026
Impact Factor: 8.2

scalability limitations inherent in single-hop point-to-point architectures, which the present work acknowledges and proposes to address in future iterations.

Kufakunesu et al. [7] examined Adaptive Data Rate (ADR) optimisation strategies for LoRaWAN networks, showing that dynamic adjustment of the spreading factor based on real-time link conditions can significantly improve network capacity. ADR integration is identified as a valuable future enhancement.

Jiang et al. [8] reviewed the opportunities and challenges of deploying LoRa networks for Agriculture 4.0 applications, covering multi-node star topology design and energy harvesting for off-grid sensor nodes. Their work reinforces the suitability of LoRa for the smart-agriculture and remote monitoring use cases targeted by this paper.

Centenaro et al. [9] provided a comprehensive overview of long-range communications in unlicensed bands, establishing the broader context within which LoRa-based IoT networks operate across smart city and industrial scenarios.

Davcev et al. [10] implemented a LoRaWAN-based IoT agriculture system demonstrating multi-node sensor deployment, providing a useful architectural reference for the multi node extension planned as future work.

III. RESEARCH GAPS IDENTIFIED

A careful review of the existing literature reveals that while LoRa-based IoT systems have been studied extensively, several important aspects remain either partially addressed or completely overlooked in practical deployments.

Gap 1 —Single-Parameter Sensing Limitation: The majority of published LoRa prototypes monitor only one physical quantity at a time, such as soil moisture, temperature, or water level [5], [10]. In safety-critical environments, multiple hazard types can occur simultaneously. Building a single LoRa architecture capable of monitoring heterogeneous sensor types within one transmission packet remains underexplored.

Gap 2 — Over-Reliance on Cloud for Alerting: Most existing implementations deliver sensor data exclusively to a cloud platform and depend entirely on internet connectivity to notify operators [2], [4]. If the network goes down, alert delivery fails silently. A reliable safety system must provide at least one alerting channel that functions completely independently of internet availability.

Gap 3 — Hardware Challenges Left Undocumented: Published research typically presents final system performance without disclosing the practical engineering difficulties encountered during hardware bring-up [3], [6]. Issues such as UART baud-rate mismatches, I2C address conflicts, GPIO voltage incompatibility, and MQ-2 sensor warm-up delays are common obstacles rarely documented.

Gap 4—India's 865 MHz ISM Band Underrepresented: Nearly all performance evaluations in LoRa literature use European (868 MHz) or North American (915 MHz) ISM allocations [1], [7]. Empirical PDR and RSSI data collected specifically within India's 865–867 MHz band remains scarce in published literature.

Gap 5 — Absence of Integrated Cost and Power Analysis: While energy efficiency is frequently cited as a key advantage of LoRa, very few works provide measured current consumption figures before and after applying low-power techniques [8]. Similarly, practical deployment cost breakdowns including component-level pricing are rarely reported.

The proposed system directly addresses all five gaps: it integrates dual-parameter sensing (Gap 1), delivers alerts through three independent output channels (Gap 2), documents every hardware challenge systematically (Gap 3), conducts all experiments within India's 865 MHz ISM band (Gap 4), and reports both measured power savings and component-level costs (Gap 5).

IV. PROPOSED SYSTEM ARCHITECTURE

The proposed system follows a two-node, single-hop wireless architecture consisting of a Sensor Transmitter Node and a Gateway Receiver Node, interconnected through a LoRa RF link. A key design principle is fault tolerance — the local alerting subsystem at the receiver operates entirely independently of internet connectivity, ensuring that threshold-

IJARSCT
International Journal of Advanced Research in Science, Communication and Technology
International Open-Access, Double-Blind, Peer-Reviewed, Refereed, Multidisciplinary Online Journal
ISSN: 2581-9429
Volume 6, Issue 2, May 2026
Impact Factor: 8.2

breach events are never suppressed by cloud or Wi-Fi unavailability. Fig. 1 illustrates the complete system architecture including data flow from sensors through the LoRa link to the cloud dashboard.

Sensor Transmitter Node

The transmitter node is built around an ESP32-WROOM 32 microcontroller, selected for its dual-core processing capability, integrated ADC channels, multiple UART peripherals, and low active power consumption. Two sensors are interfaced with this node.

The HC-SR04 ultrasonic sensor measures the distance between the sensor and the water surface, from which the water level percentage is computed using (1). The TRIG pin is connected to GPIO5 and the ECHO pin to GPIO18. Since the HC-SR04 operates at 5 V logic while the ESP32 GPIO tolerates a maximum of 3.3 V, a resistive voltage divider comprising a 10 kΩ and 20 kΩ resistor is inserted on the ECHO line to bring the signal within safe limits.

$$d = \frac{techo \times Vs}{2} \quad (1)$$

where d is the measured distance in centimetres, techo is the ECHO pulse duration in microseconds, and vs = 0.0343 cm/µs is the speed of sound at room temperature.

The MQ-2 gas sensor detects combustible gases including LPG, methane, and smoke by measuring the change in resistance of its tin dioxide (SnO2) metal oxide semiconductor sensing element when exposed to target gases. Its analogue output is connected directly to GPIO34 (ADC1 channel 6), which accepts signals up to 3.3 V. GPIO34 is a dedicated input-only pin on the ESP32 with no internal pull-up or pull-down resistor, which must be accounted for in circuit design. A mandatory 60-second warm-up period is enforced at power on to allow the MQ-2 heater element to reach its operating temperature and produce stable, accurate readings.

Sensor values are encoded into a structured ASCII payload string with the format:

NODE01|WATER|WL%|STATUS|GAS|GASVAL

where NODE01 is the node identifier, WATER is the sensor type, WL% is the water-level percentage (integer), STATUS is either HIGH or SAFE, GAS is the gas sensor identifier, and GASVAL is the concentration in ppm.

An example packet is:

NODE01|WATER|85|HIGH|GAS|450

The payload is forwarded to the RYLR998 LoRa module via UART2 on GPIO16 (TX) and GPIO17 (RX) at 115,200 baud using AT+SEND commands. The node is powered by a regulated 5 V DC supply derived from a 230 V AC mains input through a step-down transformer, 1N4007 bridge rectifier, 1000 µF filter capacitor, and LM7805 voltage regulator.

IJARSCT
International Journal of Advanced Research in Science, Communication and Technology
International Open-Access, Double-Blind, Peer-Reviewed, Refereed, Multidisciplinary Online Journal
ISSN: 2581-9429
Volume 6, Issue 2, May 2026
Impact Factor: 8.2

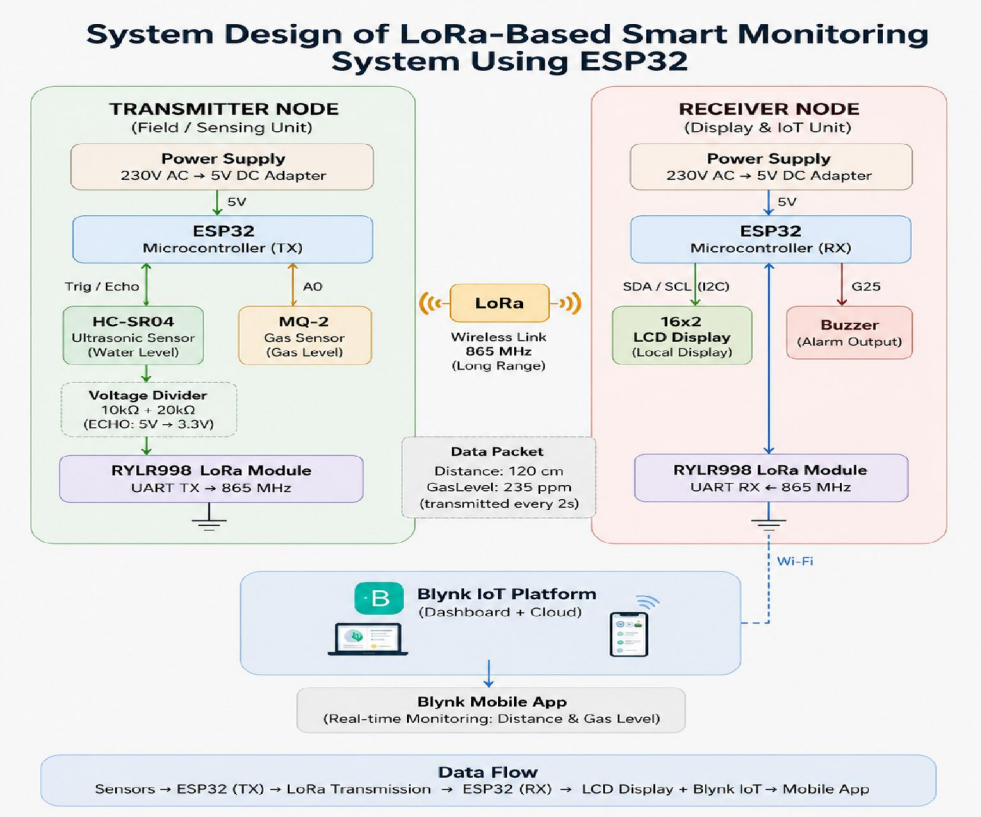

Fig. 1. System architecture of the proposed LoRa-based IoT network showing transmitter node, LoRa RF link at 865 MHz, gateway receiver, and Blynk cloud dashboard.

Receiver Node

The receiver node hosts a second ESP32-WROOM-32 paired with an RYLR998 module configured in continuous receive mode. When a valid LoRa packet arrives, the firmware parses the payload using sscanf() to extract the RSSI, SNR, and sensor values. The extracted data is then routed to three independent output channels simultaneously.

Local Display: A 16×2-character LCD with a PCF8574 I2C backpack (address 0x27) is connected on GPIO21 (SDA) and GPIO22 (SCL) with 4.7 kΩ pull-up resistors on both lines. The display shows real-time sensor readings along with a status label.

Audible Alert: An active buzzer connected to GPIO25 is triggered immediately when the water level exceeds 90% or the gas concentration exceeds 600 ppm. The water-level threshold of 90% was selected to provide a 10% safety margin before tank overflow. The gas threshold of 600 ppm was established through sensor characterisation trials to represent the lower hazard detection boundary for LPG concentrations, consistent with general industrial practice for early-warning systems. Since the buzzer operates independently of Wi-Fi or cloud connectivity, it guarantees that on-site personnel receive an alert even during network outages.

Cloud Dashboard: The ESP32's integrated Wi-Fi module connects to the Blynk IoT 2.0 platform using MQTT over WiFi. Sensor values are published to virtual pins V0 through V3, which are mapped to gauge and chart widgets on the Blynk mobile application and web console, enabling remote monitoring from any location. The receiver node is powered by an identical 230 V AC to 5 V DC regulated supply as used on the transmitter side.

IJARSCT
International Journal of Advanced Research in Science, Communication and Technology
International Open-Access, Double-Blind, Peer-Reviewed, Refereed, Multidisciplinary Online Journal
ISSN: 2581-9429
Volume 6, Issue 2, May 2026
Impact Factor: 8.2

LoRa Communication Link

Both RYLR998 modules are configured through AT commands to operate at 865 MHz, which falls within India's designated ISM band of 865–867 MHz .The link parameters are set to Spreading Factor SF9, bandwidth of 125 kHz, and coding rate 4/5. This configuration produces a nominal data rate of 976 bps.

The link budget is calculated as:

$$LB = PTX + GTX + GRX - NF - SNRmin - PL \quad (2)$$

GTX = GRX = 2.15 dBi (integrated antenna gain), NF = 6 dB (receiver noise figure), and SNRmin = −12 dB (SF9 demodulation threshold). This yields a calculated link budget exceeding 148 dB, sufficient for reliable communication beyond 1 km in semi-urban environments with mixed obstructions. A new packet is transmitted every 2 seconds, balancing data freshness against duty-cycle compliance.

V. HARDWARE AND FIRMWARE IMPLEMENTATION

Circuit Design — Transmitter Node

The transmitter circuit was designed using EasyEDA and built on a prototype perfboard. The ESP32-WROOM-32 serves as the central processing unit, interfacing with both sensors and the RYLR998 LoRa module. Since the RYLR998 operates at 3.3 V logic, it connects directly to the ESP32 UART2 pins (GPIO16/GPIO17) without requiring any additional level shifting components.

The HC-SR04 ultrasonic sensor presents a voltage compatibility challenge — its ECHO output swings to 5 V while the ESP32 GPIO input tolerates a maximum of 3.3 V. To protect the microcontroller from potential damage, a resistive voltage divider using a 10 kΩ and 20 kΩ resistor is placed on the ECHO line, bringing the signal down to approximately 3.3 V before it reaches GPIO18. The TRIG pin connects directly to GPIO5, since the HC-SR04 accepts 3.3 V logic as a valid high signal.

The MQ-2 gas sensor analogue output connects directly to GPIO34 (ADC1 channel 6). No level shifting is required here since the analogue output remains within the 0–3.3 V range under normal operating gas concentrations. The sensor is powered from the 5 V rail since its internal heater requires 5 V for proper operation.

Fig. 2 shows the transmitter circuit.

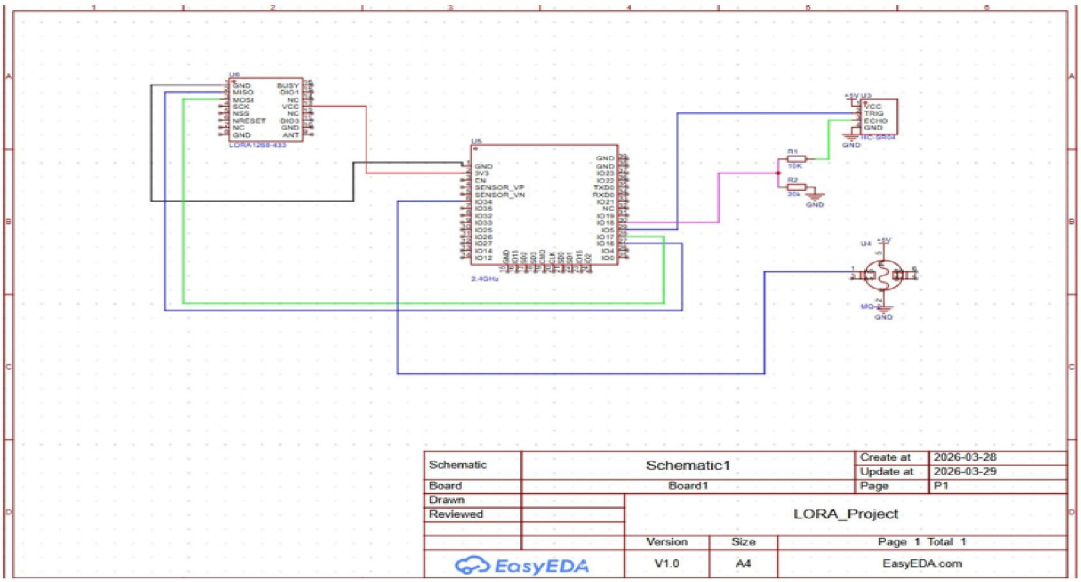

Fig. 2. Transmitter circuit showing ESP32-WROOM-32 interfaced with the RYLR998 LoRa module, HC-SR04 ultrasonic sensor (with voltage divider on ECHO line), and MQ-2 gas sensor, designed in EasyEDA.

Copyright to IJARSCT
www.ijarsct.co.in
DOI: 10.48175/IJARSCT-34877

IJARSCT
International Journal of Advanced Research in Science, Communication and Technology
International Open-Access, Double-Blind, Peer-Reviewed, Refereed, Multidisciplinary Online Journal
ISSN: 2581-9429
Volume 6, Issue 2, May 2026
Impact Factor: 8.2

Circuit Design — Receiver Node

The receiver circuit hosts the second ESP32-WROOM-32 paired with an RYLR998 in receive mode, a 16×2 I2C LCD display, and an active buzzer. Pull-up resistors of 4.7 kΩ are placed on both the SDA (GPIO21) and SCL (GPIO22) I2C lines to ensure stable communication with the PCF8574 LCD backpack at 100 kHz.

During hardware bring-up, an I2C address scan was performed to confirm the LCD backpack address. An initial conflict was encountered where the PCF8574 responded at address 0x3F instead of the expected 0x27, caused by an incorrect A0–A2 jumper configuration on the backpack board. This was resolved by verifying and correcting the solder bridge states on the PCF8574, after which the device consistently responded at 0x27.

The active buzzer is connected to GPIO25 through a transistor-based switching arrangement. Since the buzzer draws more current than the ESP32 GPIO can safely source directly, a small-signal transistor is used as a switch, with the base driven by GPIO25 through a 1 kΩ resistor and the buzzer powered from the 5 V through the transistor collector. Fig. 3 shows the receiver circuit.

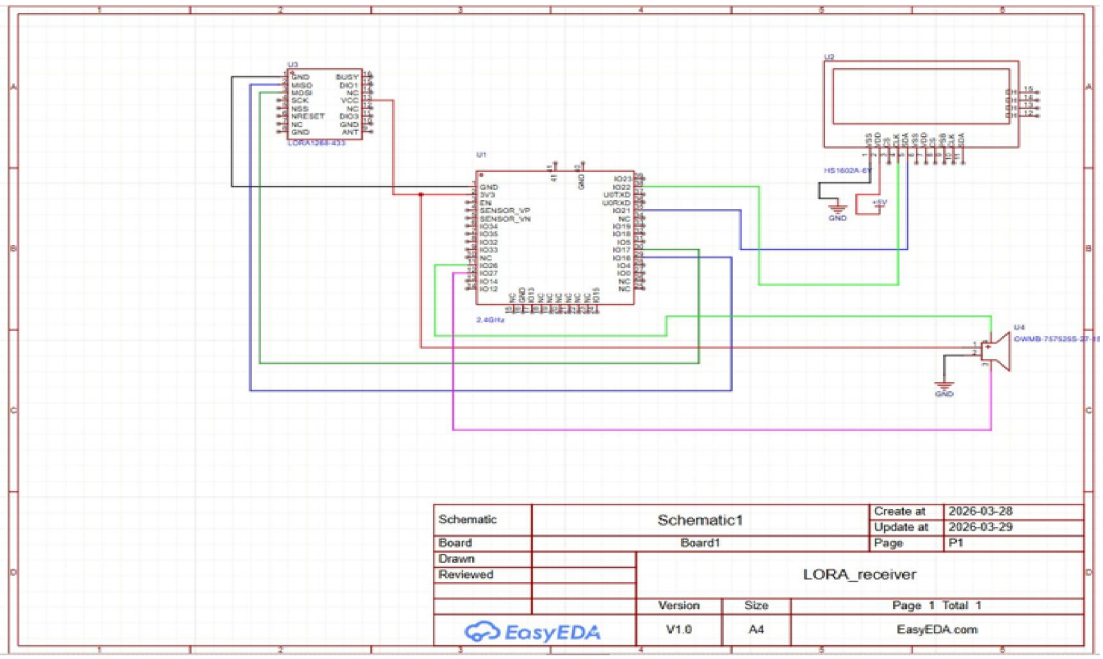

Fig. 3. Receiver circuit showing ESP32-WROOM-32 paired with RYLR998, 16×2 I2C LCD (PCF8574 backpack), and active buzzer with transistor driver, designed in EasyEDA.

Power Supply Design

Both transmitter and receiver nodes are powered by identical regulated DC supply circuits designed from the mains input. The supply circuit operates in four stages: a step-down transformer reduces 230 V AC mains to 12 V AC; a 1N4007 diode bridge rectifier converts this to pulsating DC; a 1000 µF electrolytic capacitor filters out residual ripple; and an LM7805 linear voltage regulator delivers a stable 5 V DC output at up to 1 A. The ESP32 and RYLR998 draw their 3.3 V supply from the onboard LDO regulator present on the ESP32 development board. Fig. 4 shows the power supply circuit.

IJARSCT
International Journal of Advanced Research in Science, Communication and Technology
International Open-Access, Double-Blind, Peer-Reviewed, Refereed, Multidisciplinary Online Journal
ISSN: 2581-9429
Volume 6, Issue 2, May 2026
Impact Factor: 8.2

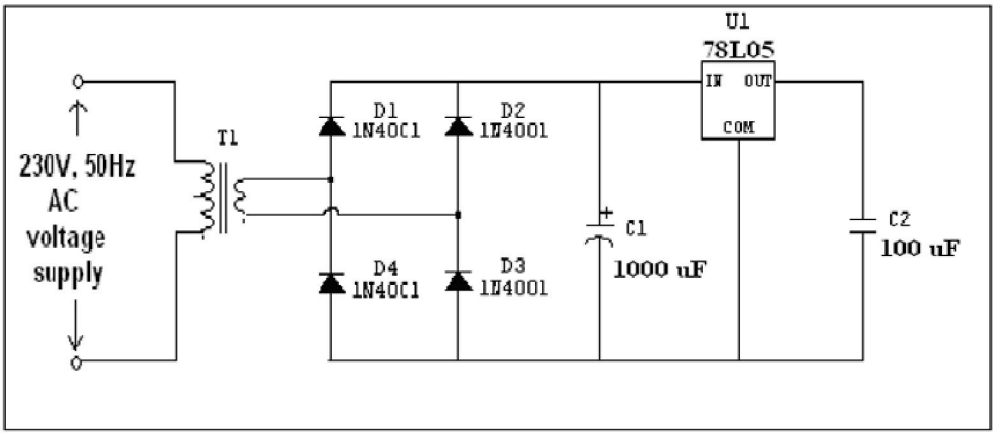

Fig. 4. Power supply circuit: 230 V AC to 5 V DC using step-down transformer, 1N4007 bridge rectifier, 1000 µF filter capacitor, and LM7805 linear voltage regulator.

Transmitter Firmware Workflow

Firmware for both nodes was developed using the Arduino framework within the Platform IO IDE on VS Code. The transmitter firmware executes the following five-stage loop on every transmission cycle.

1) Sensor Acquisition: A 10 µs pulse is issued on the HC SR04 TRIG pin. The returning ECHO pulse duration is measured using pulse In () and converted to distance using (1). The water-level percentage is computed relative to the known tank height. Simultaneously, the MQ-2 ADC value is sampled from GPIO34.

2) Gas ppm Calibration: The raw ADC reading from the MQ-2 is converted to ppm concentration using a two-point calibration curve established during sensor characterisation. A 60-second warm-up delay is enforced at power-on, allowing the MQ-2 heater element to reach thermal equilibrium and produce stable output.

3) Payload Formatting: structured the calibrated sensor values and status labels are assembled into an ASCII string of the form NODE01|WATER|WL%|STATUS|GAS|GASVAL, which allows the receiver to parse individual fields reliably using sscanf ().

4) LoRa Transmission: The formatted payload is dispatched to the RYLR998 via the AT+SEND command over UART2. If the module does not acknowledge the command within the expected time, the firmware retries transmission up to three times before logging a failure and proceeding to the next cycle.

5) Light-Sleep Entry: After a successful transmission, the ESP32 enters light-sleep mode via esp_light_sleep_start () for a 2-second interval. A millis ()-based interval check ensures the main loop remains non-blocking during normal operation. Fig. 5 shows the transmitter-side firmware workflow.

Receiver Firmware Workflow

The receiver firmware runs a continuous loop monitoring the UART buffer for unsolicited +RCV response frames generated by the RYLR998 upon successful packet reception.

1) Packet Parsing: The incoming +RCV frame is passed to sscanf (), which extracts the RSSI, SNR, payload length, and payload string. A validity check confirms that all expected fields are present before further processing begins.

2) Threshold Evaluation: Extracted sensor values are compared against configured safety thresholds. A water level above 90% sets the status to HIGH and activates the buzzer. A gas concentration above 600 ppm triggers a GAS LEAK DETECTED condition and similarly activates the buzzer.

IJARSCT
International Journal of Advanced Research in Science, Communication and Technology
International Open-Access, Double-Blind, Peer-Reviewed, Refereed, Multidisciplinary Online Journal
ISSN: 2581-9429 Volume 6, Issue 2, May 2026 Impact Factor: 8.2

3) LCD Update: The 16×2 LCD is refreshed with the latest sensor readings and their corresponding status labels on each received packet, providing continuous on-site visibility of system state.
4) Cloud Publishing: Blynk.virtualWrite() is called to push water-level, gas concentration, RSSI, and SNR values to virtual pins V0–V3 on the Blynk IoT 2.0 cloud platform, updating the mobile and web dashboard in real time.
5) Watchdog Recovery: A software watchdog timer monitors the interval since the last valid +RCV frame. If no packet is received within 5 seconds, the firmware automatically reissues an AT+RESET command to the RYLR998, recovering
the module from any transient lock-up condition without requiring manual intervention. Fig. 6 shows the receiver-side firmware workflow.

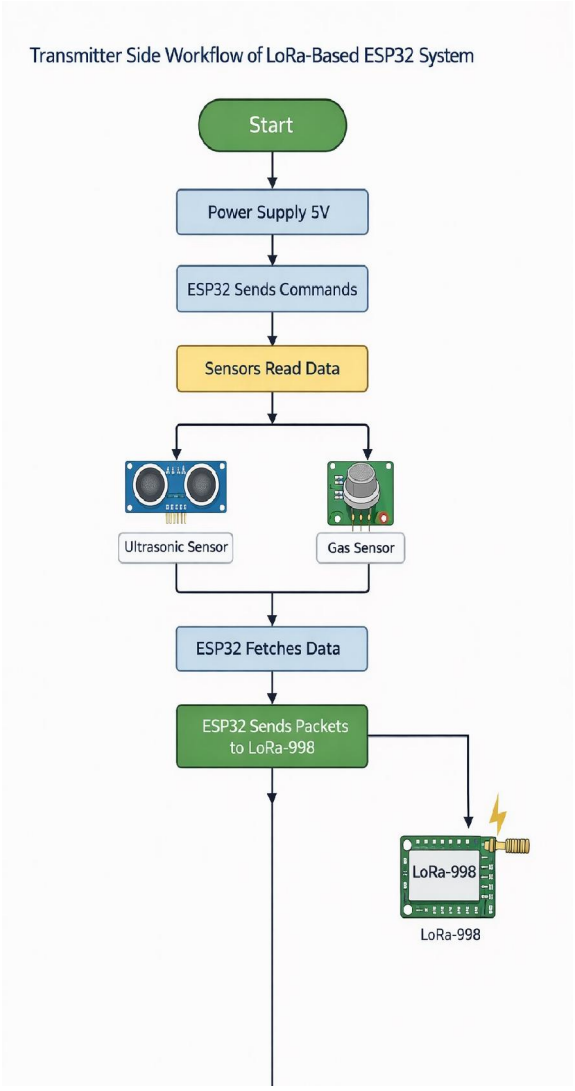

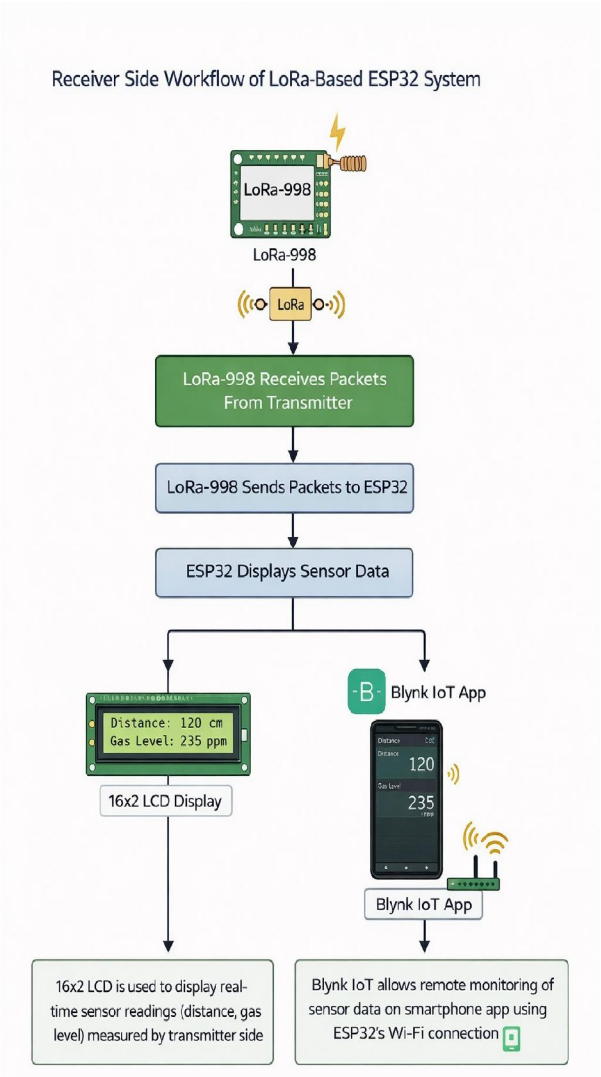

Fig. 5. Transmitter firmware workflow: sensor acquisition, gas calibration, payload formatting, LoRa transmission, and light-sleep entry.
Fig. 6. Receiver firmware workflow: packet parsing, threshold evaluation, LCD update, cloud publishing, and watchdog recovery.

IJARSCT
International Journal of Advanced Research in Science, Communication and Technology
International Open-Access, Double-Blind, Peer-Reviewed, Refereed, Multidisciplinary Online Journal
ISSN: 2581-9429
Volume 6, Issue 2, May 2026
Impact Factor: 8.2

Power Management

Minimising power consumption is essential for deployments where continuous mains power may not be available. Between transmission cycles, the ESP32 is placed into light-sleep mode using esp_light_sleep_start (), during which the CPU cores are halted but UART and GPIO peripherals remain active for wake-up. Simultaneously, the RYLR998 is commanded into its low-power standby state via AT+CPIN. Together, these measures reduce the combined node idle current from approximately 150 mA in fully active mode to approximately 9 mA — representing an 85% reduction in idle power consumption. Deep-sleep mode with RTC-triggered wake-up, which would further reduce average current consumption to below 1 mA, is identified as a future optimisation for fully off-grid battery-powered or solar-powered field deployments.

VI. EXPERIMENTAL RESULTS AND VALIDATION

The complete system was evaluated under three distinct environments to assess its communication reliability and sensor accuracy across varying propagation conditions. All tests were conducted using the same hardware prototype with fixed LoRa parameters — SF9, 125 kHz bandwidth, and coding rate 4/5. One hundred packets were transmitted in each environment, and the following metrics were recorded: Packet Delivery Ratio (PDR), Received Signal Strength Indicator (RSSI), Signal to-Noise Ratio (SNR), and end-to-end latency from sensor sampling to Blynk dashboard update.

The Packet Delivery Ratio is defined as:

$$PDR = N_{received} / N_{transmitted} \times 100\% \quad (3)$$

Test Environments

Environment 1 — Indoor Laboratory (30 m, Line of-Sight): The first trial was conducted inside the college laboratory with both nodes placed 30 m apart in a clear line-of-sight condition. This environment represented the best-case scenario with minimal obstructions and controlled RF conditions.

Environment 2 — Outdoor Open Field (500 m): The second trial was conducted in an open outdoor field with no significant obstructions between the transmitter and receiver. This represented a typical agricultural or campus deployment scenario.

Environment 3 — Semi-Urban Obstructed (1 km): The third trial was conducted across a 1 km path in a semi urban environment containing buildings, trees, and mixed obstructions. This represented the most challenging condition and tested the system's reliability under practical deployment circumstances.

Fig. 7 shows the complete assembled hardware prototype during live testing.

Link Performance Results

The system maintained a PDR above 95% across all three environments (see (3)). In the indoor line-of-sight trial, a PDR of 99.6% was recorded with strong RSSI and SNR values. As distance increased to 500 m, PDR dropped slightly to 97.8%, with RSSI declining to −96 dBm as expected from free-space path loss at 865 MHz. The semi-urban 1 km trial produced the lowest PDR of 95.3%, with the 4.7% packet loss attributed to multipath fading — consistent with observations by Liando et al. [4].

The SNR values of +7.2 dB and +3.8 dB at 500 m and 1 km respectively remain well above the SF9 demodulation threshold of approximately −12 dB, indicating a link margin of approximately 15.8 dB at 1 km. End-to-end latency remained below 380 ms across all environments, satisfying the real-time monitoring requirement.

IJARSCT
International Journal of Advanced Research in Science, Communication and Technology
International Open-Access, Double-Blind, Peer-Reviewed, Refereed, Multidisciplinary Online Journal
ISSN: 2581-9429
Volume 6, Issue 2, May 2026
Impact Factor: 8.2

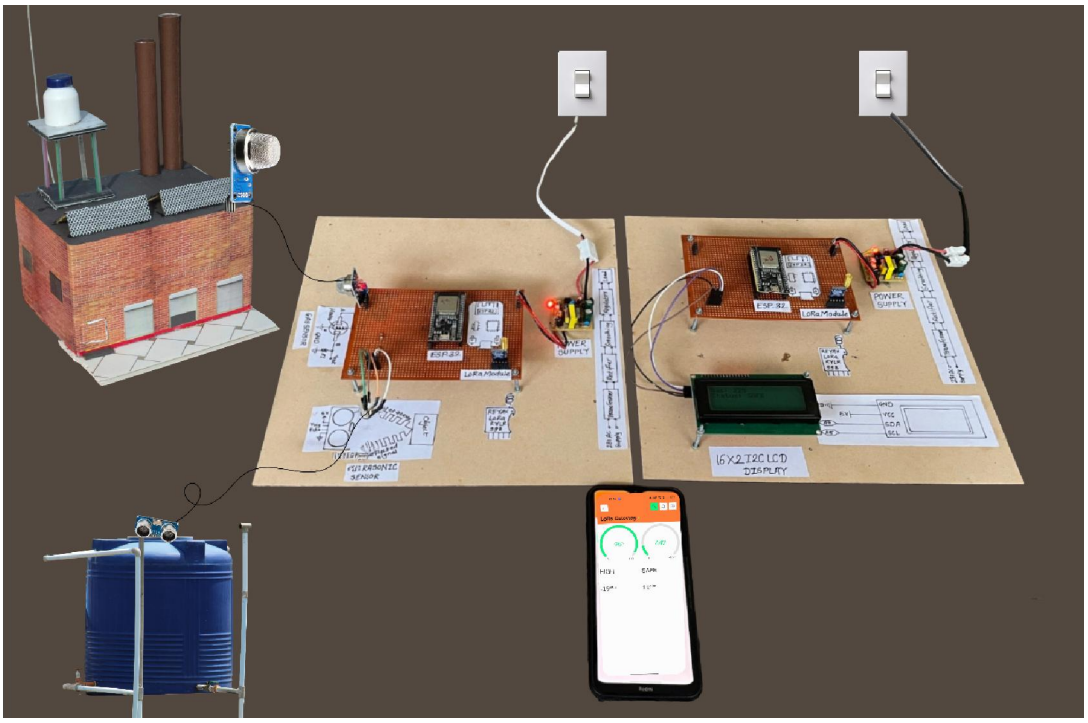

Fig. 7. Complete hardware prototype during live testing — Transmitter node (left), Receiver node with LCD display (right), and Blynk mobile app on smartphone (centre).

Sensor Accuracy Validation

Gas concentration measurements from the MQ-2 sensor were validated against a reference instrument across a range of known concentrations. The calibrated sensor produced a Mean Absolute Error (MAE) of 14 ppm at concentrations below 500 ppm, corresponding to a relative error of approximately 2.8%. This level of accuracy is adequate for threshold-based safety alerting.

Ultrasonic distance measurements from the HC-SR04 were validated by comparing sensor output against physical reference measurements at multiple known distances. Measurements showed an accuracy of ±2.4 cm up to a range of 3.5 m, consistent with manufacturer specifications.

Alert Validation

The threshold-based alerting behaviour was validated over a continuous 30-minute test session. The GAS LEAK DETECTED condition was triggered reliably every time the gas concentration exceeded 600 ppm, with no false positives recorded. The water-level HIGH alert activated correctly and consistently when the computed fill percentage crossed 90%, verified simultaneously across all three output channels — the LCD display, the active buzzer, and the Blynk cloud dashboard.

dashboard. Fig. 8 and Fig. 9 show the live LCD output during testing under HIGH water-level and SAFE gas-level conditions respectively.

Fig. 10 shows the live Blynk cloud dashboard during system operation, displaying WATER_LEVEL at 96%, WATER_STATUS as HIGH, GAS_VALUE at 409 ppm, GAS_STATUS as SAFE, RSSI of −18 dBm, and SNR of 11 dB during a close-range indoor test.

IJARSCT
International Journal of Advanced Research in Science, Communication and Technology
International Open-Access, Double-Blind, Peer-Reviewed, Refereed, Multidisciplinary Online Journal
ISSN: 2581-9429
Volume 6, Issue 2, May 2026
Impact Factor: 8.2

Fig. 8. LCD receiver output — Water level: 95%, Status: HIGH (alert triggered).

Fig. 9. LCD receiver output — Gas level: 447 ppm, Status: SAFE (normal condition).

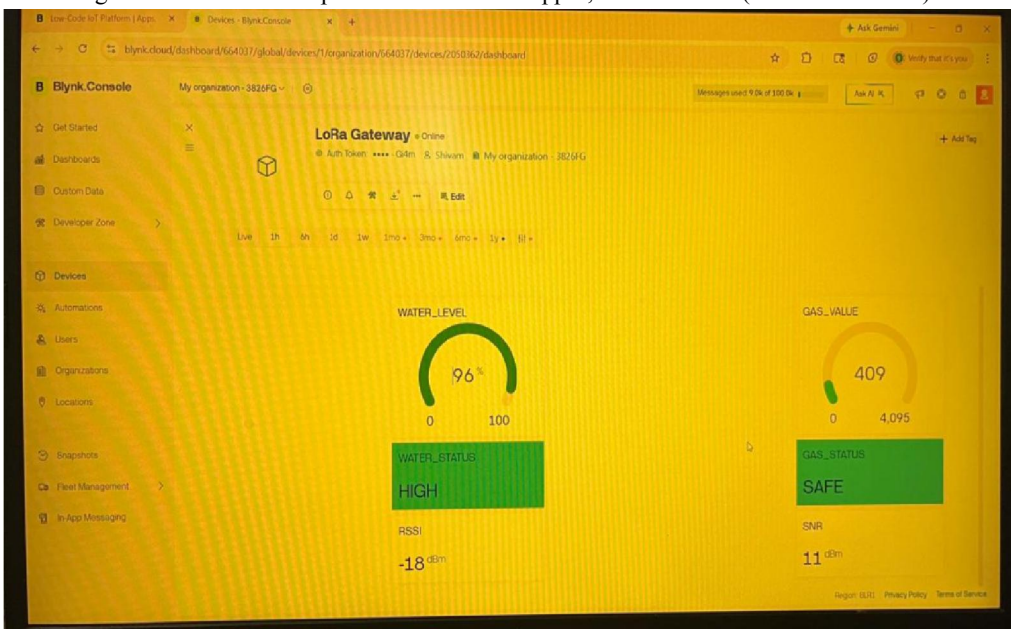

Fig. 10. Blynk IoT 2.0 cloud dashboard

IJARSCT
International Journal of Advanced Research in Science, Communication and Technology
International Open-Access, Double-Blind, Peer-Reviewed, Refereed, Multidisciplinary Online Journal
ISSN: 2581-9429
Volume 6, Issue 2, May 2026
Impact Factor: 8.2

VII. DISCUSSION

Communication Reliability

The experimental results demonstrate that LoRa point-to point communication at 865 MHz provides dependable wireless connectivity across all three tested environments without relying on any existing network infrastructure. Maintaining a PDR above 95% at distances up to 1 km in a semi-urban environment confirms that the RYLR998 module configured at SF9 is well-suited for the target deployment scenarios of smart agriculture, campus monitoring, and industrial safety applications.

The observed decline in PDR from 99.6% at 30 m to 95.3% at 1 km follows a predictable pattern consistent with increasing multipath fading at greater distances, as documented in large-scale LoRa evaluations by Liando et al. [4]. The SNR values recorded at all distances remained well above the SF9 demodulation threshold, indicating the system still operates with a comfortable link margin.

The RYLR998 AT-command interface proved to be a significant practical advantage during firmware development. Compared to direct SPI-based integration with raw LoRa chips, the AT-command abstraction allowed the transmitter and receiver firmware to be developed, debugged, and validated in a shorter time. The trade-off is that this abstraction restricts access to advanced MAC-layer features such as adaptive data rate, which are available in full LoRaWAN stacks [7].

Effectiveness of Tri-Modal Alerting

One of the central design decisions of this work was to deliver alerts through three independent output channels rather than relying exclusively on cloud connectivity. The experimental validation confirmed that this approach works effectively in practice. When sensor thresholds were breached during testing, the buzzer activated within tens of milliseconds of the packet being received, the LCD updated immediately, and the Blynk dashboard reflected the alert within the measured end-to-end latency of under 380 ms.

The importance of this independence becomes clear when considering failure scenarios. A Wi-Fi outage, a Blynk server interruption, or a mobile data connectivity issue would completely silence a cloud-only alerting system. In the proposed architecture, the buzzer and LCD continue to function regardless of internet availability. This directly addresses Gap 2 identified in Section III and represents the most practically significant contribution of this work for safety-critical deployments.

Hardware Integration Challenges

Several hardware challenges were encountered and resolved during system development, each of which carries practical lessons for embedded IoT practitioners.

The voltage incompatibility between the HC-SR04 ECHO output (5 V) and the ESP32 GPIO input (3.3 V maximum) is a common issue frequently overlooked in prototype designs. Without the resistive voltage divider, sustained 5 V exposure on the ESP32 GPIO pin risks permanent damage to the microcontroller.

The I2C address conflict on the PCF8574 LCD backpack, where the device initially responded at 0x3F due to an A0 A2 jumper misconfiguration, is another issue commonly encountered but rarely documented. The resolution — verifying and correcting the solder bridge states — is straightforward once the root cause is identified but can consume significant debugging time without prior knowledge.

The MQ-2 sensor warm-up requirement of 60 seconds is critical for measurement accuracy. Readings taken before the heater element reaches thermal equilibrium produce unreliable ppm values that could either trigger false alarms or miss genuine hazards.

Limitations

The current single-hop, point-to-point architecture imposes a fundamental scalability constraint. Adding a third sensor node would require either dedicated frequency separation or time-division scheduling, since the RYLR998 does not

IJARSCT
International Journal of Advanced Research in Science, Communication and Technology
International Open-Access, Double-Blind, Peer-Reviewed, Refereed, Multidisciplinary Online Journal
ISSN: 2581-9429 Volume 6, Issue 2, May 2026 Impact Factor: 8.2

implement MAC-layer collision avoidance. This limits the architecture to small deployments and motivates the LoRaWAN upgrade described below.

The Blynk IoT 2.0 cloud platform, while enabling rapid mobile dashboard development, is a proprietary service. Industrial deployments requiring data sovereignty or offline operation would be better served by an open-source MQTT broker such as Eclipse Mosquitto paired with a Grafana visualisation layer [6].

The HC-SR04 ultrasonic sensor is sensitive to temperature variation and surface turbulence, both of which can introduce measurement error beyond the ±2.4 cm baseline accuracy. A temperature-compensated ultrasonic sensor or a pressure-based level sensor would improve reliability in outdoor deployments.

Future Work

Several enhancements are planned to extend the capabilities of the current prototype:

- Multi-node LoRaWAN deployment: Migration to a star topology LoRaWAN network using a Raspberry Pi-based gateway connected to The Things Network (TTN) will enable addressable management of multiple sensor nodes with adaptive data rate support [6].
- Deep-sleep power optimisation: Implementing deep sleep with RTC-triggered wake-up is projected to reduce average current consumption to below 1 mA, enabling fully off-grid solar-powered field deployment.
- Open-source cloud migration: Replacing the Blynk platform with Eclipse Mosquitto and Grafana will provide on-premises data storage, offline resilience, and full data sovereignty.
- AI-based predictive monitoring: Integrating a machine learning model trained on historical sensor trends to forecast hazardous conditions before threshold breach, enabling proactive safety intervention aligned with Industry 4.0 objectives [8].
- Additional sensor integration: Expanding the sensor suite to include temperature, humidity, and soil moisture parameters will broaden applicability to comprehensive smart agriculture deployments.

VIII. CONCLUSION

This paper presented the design, hardware implementation, firmware development, and experimental field validation of a LoRa-based IoT network for real-time environmental monitoring and safety alerting. The system was built around two ESP32-WROOM-32 microcontroller nodes communicating wirelessly through RYLR998 LoRa transceivers operating at India's 865 MHz ISM band, integrating water-level sensing via an HC-SR04 ultrasonic sensor and combustible gas detection via an MQ-2 metal oxide semiconductor gas sensor within a single two-node architecture.

Field evaluation across three environments demonstrated that the system maintains a Packet Delivery Ratio exceeding 95% at distances up to 1 km in semi-urban obstructed conditions, with end-to-end latency consistently below 380 ms from sensor sampling to Blynk cloud dashboard update. The measured SNR values at all tested distances remained well above the SF9 demodulation threshold, confirming a link margin of approximately 15.8 dB at 1 km.

The tri-modal output architecture — combining a 16×2 I2C LCD display, a threshold-triggered active buzzer, and a Blynk IoT 2.0 cloud dashboard — ensures that safety-critical alerts are delivered through independent channels that do not share a common point of failure.

Hardware integration challenges encountered during development — including UART baud-rate synchronisation, I2C address conflicts on the PCF8574 LCD backpack, GPIO voltage incompatibility between 5 V sensors and 3.3 V microcontroller pins, and MQ-2 sensor warm-up management — were systematically resolved and documented as a practical engineering reference.

The complete two-node system was realised at a total component cost of Rs. 6,543. Power management through ESP32 light-sleep and RYLR998 low-power mode reduced idle current consumption by 85%, from approximately 150 mA to 9 mA. The proposed architecture is scalable, energy efficient, and directly applicable to smart agriculture, campus IoT monitoring, industrial gas-hazard detection, and water resource management.

IJARSCT
International Journal of Advanced Research in Science, Communication and Technology
International Open-Access, Double-Blind, Peer-Reviewed, Refereed, Multidisciplinary Online Journal
ISSN: 2581-9429
Volume 6, Issue 2, May 2026
Impact Factor: 8.2

ACKNOWLEDGMENT

The authors gratefully acknowledge the Department of Electronics and Telecommunication Engineering, Late G. N. Sapkal College of Engineering, Nashik, for providing laboratory facilities and hardware resources essential to the completion of this work. Special recognition is extended to Prof. S. G. Bagul, Assistant Professor, for sustained technical mentorship, guidance on experimental methodology, and continuous encouragement throughout the duration of this project.

REFERENCES

[1] Semtech Corporation, "LoRa Modulation Basics," Application Note AN1200.22, Rev. 2, May 2015.
[2] A. Augustin, J. Yi, T. Clausen, and W. M. Townsley, "A Study of LoRa: Long Range and Low Power Networks for the Internet of Things," Sensors, vol. 16, no. 9, p. 1466, Sep. 2016. https://doi.org/10.3390/ s16091466
[3] U. Raza, P. Kulkarni, and M. Sooriyabandara, "Low Power Wide Area Networks: An Overview," IEEE Communications Surveys & Tutorials, vol. 19, no. 2, pp. 855–873, Q2 2017.
[4] J. C. Liando, A. Gamage, A. W. Tengourtius, and M. Li, "Known and Unknown Facts of LoRa: Experiences from a Large-Scale Measurement Study," ACM Transactions on Sensor Networks, vol. 15, no. 2, pp. 1–35, Feb. 2019.
[5] M.A.Islam, L. M. Dang, S. Baik, and H. Moon, "IoT-Based Water Level Monitoring System Using LoRa Communication," International Journal of Advanced Computer Science and Applications (IJACSA), vol. 11, no. 3, 2020. [6] J. P.Shanmuga Sundaram, W. Du, and Z. Zhao, "A Survey on LoRa Networking: Research Problems, Current Solutions and Open Issues," IEEE Communications Surveys and Tutorials, vol. 22, no. 1, pp. 371 388, 2020.
[7] R. Kufakunesu, G. P. Hancke, and A. M. Abu-Mahfouz, "A Survey on Adaptive Data Rate Optimisation in LoRaWAN: Recent Solutions and Open Issues," MDPI Sensors, vol. 20, no. 3, article 822, 2020.
[8] Z. Jiang, Y. He, B. Luo, and H. Du, "LoRa Communication for Agri culture 4.0: Opportunities, Challenges, and Future Directions," arXiv preprint arXiv:2409.11200, Sep. 2024.
[9] M. Centenaro, L. Vangelista, A. Zanella, and M. Zorzi, "Long-Range Communications in Unlicensed Bands: The Rising Stars in the IoT and Smart City Scenarios," IEEE Wireless Communications, vol. 23, no. 5, pp. 60–67, Oct. 2016. https://ieeexplore.ieee.org/document/7823340
[10] D. Davcev, K. Mitreski, S. Trajkovic, V. Nikolovski, and N. Koteli, "IoT Agriculture System Based on LoRaWAN," in Proc. IEEE 14th International Workshop on Factory Communication Systems (WFCS), Imperia, Italy, Jun. 2018, pp. 1–4.
[11] Espressif Systems, "ESP32 Technical Reference Manual," Ver. 5.1, 2023. [Online]. Available: https://www.espressif.com
[12] Blynk Inc., "Blynk IoT Platform Documentation," 2024. [Online]. Available: https://docs.blynk.io